Chemical trends and bonding mechanisms for isolated adsorbates on Al(111)

J. Bormet,* J. Neugebauer,† and M. Scheffler
Fritz-Haber-Institut der Max-Planck-Gesellschaft, Faradayweg 4-6, D-14 195 Berlin-Dahlem, Germany
(Received 13 December 1993)

Using the self-consistent surface-Green-function method we study the chemisorption of isolated adatoms bonded to the (111) surface of aluminum. In order to identify chemical trends, a group-I, group-IV, and group-VII adsorbate is considered. Our study is analogous to that of Lang and Williams with the difference that their substrate was jellium, whereas we take the substrate atomic structure fully into account. The influence of the atomic structure is clearly noticeable in the electronic density of states, charge density, and atomic geometry, but the main (qualitative) conclusions of Lang and Williams are supported by our results. The discussion of the group-I adsorbate is complemented by calculations for periodic adlayers, in order to demonstrate the influence of adsorbate-adsorbate interactions.

I. INTRODUCTION

The understanding of the chemisorption bond of isolated adsorbates on surfaces is fundamental to the study of more complex phenomena such as chemical reactions and catalytic effects on surfaces. A systematic investigation for different adatoms was performed in pioneering work by Lang and Williams,[1] in which they describe total-energy and electronic structure calculations for different atoms adsorbed on a jellium substrate. Thus, the atomic structure of the substrate is replaced by a structureless, positive charge density which at the surface goes abruptly to zero. They use a substrate with a density parameter $r_s = 2$ in order to model aluminum. Recently it became quite clear, however, that Al is not free-electron-like. For example, the top layer of Al(111) relaxes slightly outward, i.e., not inward as it should for a free-electron metal, and the work function of Al(111) is smaller than that of the (100) surface.[2] Both effects result from the Al band structure (i.e., from the tendency of Al towards covalence), as is the fact that adatoms are sometimes adsorbed substitutionally.[3–5,7] A further clear indication of the importance of the Al atomic structure for surface properties is that a neglect of the atomic structure, i.e., the jellium approach for Al, gives a negative surface energy.[8] Thus, the basic fact that an Al crystal and its surface exist at all is crucially determined by the atomic structure and its influence on the electronic energy bands.

Using our self-consistent surface-Green-function (SSGF) method (see Ref. 9 and Sec. II below) we investigated the same chemisorption systems as Lang and Williams in order to determine the influence of the atomic structure of the substrate on the chemisorption process. A Green-function method was applied as it gives an accurate and most efficient description for *isolated* adsorbates on a semi-infinite substrate. This approach takes advantage of the fact that the adsorbate induced perturbation of the charge density and the change of the potential (but not the adsorbate wave functions) are localized in real space. When the Green function of the clean substrate is known, the adsorbate geometry, charge density, and binding energy can be calculated efficiently via the Dyson equation requiring information only inside a rather small region around the adsorbate.

In view of a comparison with the jellium calculations of Lang and Williams, we study the low-coverage case assuming that the adsorbate sits on the unrelaxed Al(111) surface in the highest coordinated site, which is the hollow position. For low coverages this is indeed the stable geometry and the substrate relaxation is very small.[5,6] Investigating single adatoms implies that we can identify the pure adsorbate-substrate interaction. At higher coverages, changes of the adsorbate dipole moment, adsorbate position, substrate reconstruction, and phase transitions into islands may occur.[4,5,7] These effects are either due to an adsorbate-adsorbate interaction or they require some activation energy and are therefore not considered in this paper.

The outline of this paper is as follows. In Sec. II we briefly describe our Green-function method; in particular, we derive the expressions for the total energy and the forces on atoms. In Sec. III we investigate the chemical trends of several quantities which are characteristic of chemisorption systems, such as the adsorption geometry, density of states, and charge density. Agreement with and differences from the results of Lang and Williams are discussed. Section IV concentrates on some aspects concerning the charge transfer between adsorbate and substrate, and in Sec. V the transition from low coverages to high coverages is discussed. Finally, in Sec. VI we summarize the results.

II. THE SELF-CONSISTENT SURFACE-GREEN-FUNCTION METHOD

Our self-consistent surface-Green-function method is described in Ref. 9, where the emphasis was put on electronic structure calculations. In this section we extend

this work and describe the evaluation of total energies and forces.

Simply put, our method may be viewed as a successor to the self-consistent "defect Green-function method"[10–14] which was developed around 1980 and was successfully applied to many defects in semiconductors. Besides taking ideas from the defect Green-function method, the SSGF method is based on the layer–Korringa-Kohn-Rostoker (KKR) Green-function formalism,[15] combining it with *ab initio* pseudopotential theory.[16–19] Alternative methods have been developed by Dederichs, Zeller, and co-workers,[20,21] Gunnarsson, Jepsen, and Andersen,[22] Beeler, Andersen, and Scheffler,[23] and Feibelman and co-workers.[24–26]

It is useful to split the Hamilton operator of the total system into two parts:

$$\mathcal{H} = \mathcal{H}^0 + \Delta V^{\rm eff} \quad . \tag{1}$$

The "reference system" $\mathcal{H}^0 = -\frac{1}{2}\nabla^2 + V^0$ describes the semi-infinite substrate for a given potential V^0. Throughout this paper equations are given in Hartree atomic units. For the calculations reported below, we have used a potential V^0 which is self-consistent in the bulk region and has a step barrier at the surface. The barrier height is given by the bulk Fermi level and the work function. The latter is obtained from a self-consistent slab calculation[4] which gives $\Phi = 4.2$ eV. Measured from the muffin-tin zero our height of the surface barrier is 13.1 eV. We use *ab initio,* ionic pseudopotentials[18] and denote the valence-electron density of this model substrate, which is produced by the Hamiltonian $\mathcal{H}^0$, as $n^{\rm v,0}(\mathbf{r})$. Because the potential V^0 is not self-consistent at the surface, $V^{\rm eff} = V^0 + \Delta V^{\rm eff}$ is the effective potential of the adsorbate system accounting not only for the adsorbed atom but also for the contributions which describe the difference between V^0 and a self-consistent substrate surface.

Splitting the Hamiltonian as in Eq. (1) becomes highly advantageous if an *operator* Green-function method is applied that treats the operator of the kinetic energy only in the "reference system" $\mathcal{H}^0$. Another advantage of the Green-function method follows from the effective and highly localized screening properties of metals. As a consequence, $\Delta V^{\rm eff}$ is well localized in real space, which enables accurate and efficient calculations. We emphasize that, while $\Delta V^{\rm eff}$ is well localized, the wave functions of the adsorbate system can be (and typically are) extended.

For the *change* in the effective potential of the adsorbate system we write

$$\Delta V^{\rm eff}[n^{\rm v}] = V^{\rm eff}[n^{\rm v}] - V^0 \quad , \tag{2}$$

where $n^{\rm v}(\mathbf{r})$ is the density of the valence electrons, and $V^{\rm eff}[n^{\rm v}]$ is the functional of the effective potential as defined by the Kohn-Sham equation. When the potential of the ions of the reference system is denoted by $V^{\rm ion,0}$ and when we define

$$\Delta V^{\rm eff,sc0} = V^{\rm ion,0} + V^{\rm Hartree}[n^{\rm v,0}] + V^{\rm xc}[n^{\rm v,0}] - V^0 \quad , \tag{3}$$

we obtain the following equation:

$$\Delta V^{\rm eff}[n^{\rm v}] = \Delta V^{\rm ion} + \Delta V^{\rm Hartree}[n^{\rm v}] + \Delta V^{\rm xc}[n^{\rm v}] + \Delta V^{\rm eff,sc0} \quad . \tag{4}$$

Here the different terms on the right are the changes in the ionic potential, the Hartree potential, $\Delta V^{\rm Hartree}[n^{\rm v}] = V^{\rm Hartree}[n^{\rm v}(\mathbf{r}) - n^{\rm v,0}(\mathbf{r})]$, and the exchange-correlation potential, $\Delta V^{\rm xc}[n^{\rm v}] = V^{\rm xc}[n^{\rm v}(\mathbf{r})] - V^{\rm xc}[n^{\rm v,0}(\mathbf{r})]$. In the actual calculations the functional $V^{\rm xc}[n(\mathbf{r})]$ is evaluated using the local-density approximation. The ionic potentials are described in the frozen-core approximation. For an adatom at the surface and a rigid substrate $\Delta V^{\rm ion}$ then is the ionic potential (nucleus plus core electrons) of the free adatom. When lattice relaxations are taken into account, $\Delta V^{\rm ion}$ also includes the changes due to a displacement of substrate ions. The last term in Eq. (4) [i.e., Eq. (3)] accounts for the fact that the theoretical description of the clean substrate surface, i.e., the potential V^0, need not be self-consistent. Obviously, if V^0 were a self-consistent potential then $\Delta V^{\rm eff,sc0}$ would vanish.

The Green-function operator of the reference system at complex energy $Z = \epsilon + i\eta$,

$$\mathcal{G}^0(Z) = \left(Z - \mathcal{H}^0\right)^{-1} \quad , \tag{5}$$

is calculated using the layer-KKR method.[15] This gives a highly accurate description of its real as well as its imaginary parts. For the difference of $\mathcal{G}(Z)$ and $\mathcal{G}^0(Z)$ we obtain

$$\Delta\mathcal{G}(Z) = \mathcal{G}(Z) - \mathcal{G}^0(Z) = \mathcal{G}^0(Z)\Delta V^{\rm eff}\left(\boldsymbol{I} - \mathcal{G}^0(Z)\Delta V^{\rm eff}\right)^{-1}\mathcal{G}^0(Z) \quad . \tag{6}$$

The quantity of interest is the electron-density change, $\Delta n^{\rm v}(\mathbf{r}) = n^{\rm v}(\mathbf{r}) - n^{\rm v,0}(\mathbf{r})$, induced by the adsorbate system and it is obtained from $\mathrm{Im}\,\Delta\mathcal{G}(Z)$. We make the following (general) ansatz for this quantity in a localized basis:

$$\Delta n^{\rm v}(\mathbf{r}) = \sum_{i,j} \Delta n^{\rm v}_{i,j}\,\chi_i(\mathbf{r})\chi^*_j(\mathbf{r}) \quad , \tag{7}$$

where the set $\{\chi_i(\mathbf{r})\}$ contains orthonormal localized basis functions. For details we refer to Ref. 9. For the calculations reported below, the function space $\{\chi_i(\mathbf{r})\}$ is constructed from s, p, and d gaussians which are centered at the adatom and its three neighbor Al atoms. For each angular quantum number we use three gaussians having different decays ($\alpha = 0.15$, 0.38, and 0.6 bohr^{-2} for the Na and Si adsorbate systems, and $\alpha = 0.15$, 0.5, and 1.0 bohr^{-2} for the Cl adsorbate system). Several test calculations with different decays showed that this basis of 108 linearly independent functions is sufficiently flexible to represent the two localized functions $\Delta n^{\rm v}(\mathbf{r})$ and $\Delta V^{\rm eff}(\mathbf{r})$.

Once the change of the valence-electron density $\Delta n^{\rm v}(\mathbf{r})$ is calculated self-consistently we can evaluate the total energy. The total-energy functional for the valence-electron density $n^{\rm v}(\mathbf{r})$, which describes *all* the valence

electrons of the substrate and the adsorbate, can be written as

$$E^{\rm tot}[n^{\rm v}] = \sum_i^{\rm occ} \epsilon_i^{\rm v,out} + \frac{1}{2}\int\int \frac{n^{\rm v,out}(\mathbf{r})n^{\rm v,out}(\mathbf{r}')}{|\mathbf{r}-\mathbf{r}'|}d^3r d^3r' - \int\int \frac{n^{\rm v,out}(\mathbf{r})n^{\rm v,in}(\mathbf{r}')}{|\mathbf{r}-\mathbf{r}'|}d^3r d^3r' + \int \left[n^{\rm v,out}(\mathbf{r}) + n^{\rm c,at}(\mathbf{r})\right]\epsilon^{\rm xc}[n^{\rm v,out}(\mathbf{r}) + n^{\rm c,at}(\mathbf{r})]d^3r - \int n^{\rm v,out}(\mathbf{r})V^{\rm xc}[n^{\rm v,in}(\mathbf{r}) + n^{\rm c,at}(\mathbf{r})]d^3r + \frac{1}{2}{\sum_{k,l}}' \frac{Z_k^{\rm v}Z_l^{\rm v}}{|\mathbf{R}_k - \mathbf{R}_l|} + \epsilon_F \Delta Q \quad . \tag{8}$$

The superscripts "out" and "in" indicate whether the corresponding quantity is taken as "input" or "output" for the Kohn-Sham equation (in our case the corresponding Dyson equation). The distinction between $n^{\rm v,in}$ and $n^{\rm v,out}$ is necessary in order to take full advantage of the variational principle of the total energy. The $\epsilon_i^{\rm v}$ are the single-particle eigenvalues of the valence electrons and ϵ_F is the Fermi level. $\epsilon^{\rm xc}$ is the exchange-correlation energy per electron and is taken in the local-density approximation (LDA).[27] Although we use *ab initio* pseudopotentials,[18] we (usually) do not linearize the exchange-correlation interaction of core and valence electrons. This implies that the electron density of the frozen (atomic) core states, $n^{\rm c,at}(\mathbf{r})$, appears in Eq. (8). The contribution $\frac{1}{2}{\sum_{k,l}}' \frac{Z_k^{\rm v}Z_l^{\rm v}}{|\mathbf{R}_k-\mathbf{R}_l|}$ is the electrostatic interaction of the positive ions.

The last term $\epsilon_F \Delta Q$ accounts for the fact that our Green-function method uses a constant chemical potential ϵ_F, the Fermi level of the substrate bulk. Thus, there is no explicit constraint for charge neutrality in the system. The net charge of the system in the region of integrations $\Omega^{\rm loc}$ in which $\Delta n^{\rm v}(\mathbf{r})$ is different from zero is denoted by ΔQ. Although we do not force the system to become neutral, the nature of the metallic screening implies that in all practical cases we have studied, ΔQ was smaller than one-hundredth of an electron, which is a confirmation that the function space $\{\chi_i(\mathbf{r})\}$ is sufficiently flexible.

The total energy of the adsorbate system can be evaluated by considering only a finite, and typically very small, region $\Omega^{\rm loc}$. This is true because all the kernels of the integrals in Eq. (8) can be factorized into products of two quantities one of which is strongly localized in the spatial region $\Omega^{\rm loc}$. Furthermore, we evaluate the energy summation in the complex energy plane along the following energy contour: $\Gamma^{\epsilon} \equiv (\epsilon^{\rm bot},0) \rightarrow (\epsilon^{\rm bot},1\,{\rm eV}) \rightarrow (\epsilon_F,1\,{\rm eV}) \rightarrow (\epsilon_F,0)$. Here $\epsilon^{\rm bot}$ is an energy below the lowest occupied valence state. The change of the total energy of the adsorbate system is

$$\begin{aligned}
\Delta E^{\rm tot} = {} & \frac{2}{\pi}\left[\epsilon_F\delta(\epsilon_F) - \epsilon^{\rm bot}\delta(\epsilon^{\rm bot})\right] - \frac{2}{\pi}\left\{\oint_{\Gamma^{\epsilon}}\delta(Z)dZ\right\} \\
& + \frac{1}{2}\int_{\Omega^{\rm loc}}\Delta n^{\rm v,out}(\mathbf{r})\left[\int_{\Omega^{\rm loc}}\frac{\Delta n^{\rm v,out}(\mathbf{r}') - n^{\rm tst,out}(\mathbf{r}')}{|\mathbf{r}-\mathbf{r}'|}d^3r' + V^{\rm tst,out}(\mathbf{r})\right]d^3r \\
& - \int_{\Omega^{\rm loc}}\Delta n^{\rm v,out}(\mathbf{r})\left[\int_{\Omega^{\rm loc}}\frac{\Delta n^{\rm v,in}(\mathbf{r}') - n^{\rm tst,in}(\mathbf{r}')}{|\mathbf{r}-\mathbf{r}'|}d^3r' + V^{\rm tst,in}(\mathbf{r})\right]d^3r \\
& + \int_{\Omega^{\rm loc}}\left[\sum_{a=1}^{N^{\rm ad}} n_a^{\rm ion}(|\mathbf{r}-\mathbf{R}_a|)\right]\left[\int_{\Omega^{\rm slab}}\frac{\left[\sum_{a=N^{\rm ad}+1}^{\infty} n_a^{\rm ion}(|\mathbf{r}'-\mathbf{R}_l|)\right] - n^{\rm v,0}(\mathbf{r}')}{|\mathbf{r}-\mathbf{r}'|}d^3r'\right]d^3r \\
& + \int_{\Omega^{\rm loc}}\left[{\rm Im}\left\{\sum_{i,j} n_{ij}^{\rm v,0}\chi_i(\mathbf{r})\chi_j^*(\mathbf{r})\right\}\right] \\
& \times \left[\int_{\Omega^{\rm loc}}\frac{\sum_{a=1}^{N^{\rm ad}} n_a^{\rm ion}(|\mathbf{r}-\mathbf{R}_a|)}{|\mathbf{r}-\mathbf{r}'|}d^3r' + \int_{\Omega^{\rm loc}}\frac{n^{\rm tst,in}(\mathbf{r}') - \Delta n^{\rm v,in}(\mathbf{r}')}{|\mathbf{r}-\mathbf{r}'|}d^3r' - V^{\rm tst,in}(\mathbf{r})\right]d^3r \\
& + \int_{\Omega^{\rm loc}}\left[\Delta n^{\rm v,out}(\mathbf{r}) + n^{\rm v,0}(\mathbf{r}) + n^{\rm c,at}(\mathbf{r})\right] \\
& \times \left\{\epsilon^{\rm xc}[\Delta n^{\rm v,out}(\mathbf{r}) + n^{\rm v,0}(\mathbf{r}) + n^{\rm c,at}(\mathbf{r})] - \epsilon^{\rm xc}[n^{\rm v,0}(\mathbf{r}) + n^{\rm c,at,0}(\mathbf{r})]\right\}d^3r \\
& + \int_{\Omega^{\rm loc}}\left[\Delta n^{\rm v,out}(\mathbf{r}) + \Delta n^{\rm c,at}(\mathbf{r})\right]\epsilon^{\rm xc}[n^{\rm v,0}(\mathbf{r}) + n^{\rm c,at,0}(\mathbf{r})]d^3r \\
& - \int_{\Omega^{\rm loc}}\left[\Delta n^{\rm v,out}(\mathbf{r}) + n^{\rm v,0}(\mathbf{r})\right] \\
& \times \left\{V^{\rm xc}[\Delta n^{\rm v,in}(\mathbf{r}) + n^{\rm v,0}(\mathbf{r}) + n^{\rm c,at}(\mathbf{r})] - V^{\rm xc}[n^{\rm v,0}(\mathbf{r}) + n^{\rm c,at,0}(\mathbf{r})]\right\}d^3r \\
& - \int_{\Omega^{\rm loc}}\Delta n^{\rm v,out}(\mathbf{r})V^{\rm xc}[n^{\rm v,0}(\mathbf{r}) + n^{\rm c,at,0}(\mathbf{r})]d^3r + \sum_{a=1}^{N^{\rm ad}}\sum_{b=a+1}^{N^{\rm ad}}\frac{Z_a^{\rm v}Z_b^{\rm v}}{|\mathbf{R}_a - \mathbf{R}_b|} + \epsilon_F\Delta Q
\end{aligned} \tag{9}$$

The spatial region $\Omega^{\rm slab}$ has the planar translational symmetry of the reference system and a thickness of several crystal layers plus some vacuum region. There should be at least as many layers as there are in $\Omega^{\rm loc}$. In Eq. (9) there are some new symbols which are not defined so far. $n^{\rm c,at,0}(\mathbf{r})$ is the density of the core electrons of the clean substrate. The generalized phase shifts are defined as

$$\delta(Z) = -\mathrm{Im}\ln\det[\boldsymbol{I} - \mathcal{G}^0(Z)\Delta V^{\rm eff}] \quad , \tag{10}$$

with $\boldsymbol{I}$ being the unity matrix. $N^{\rm ad}$ denotes the (finite) number of adsorbate atoms (below we have $N^{\rm ad} = 1$), and $n_a^{\rm ion}(\mathbf{r})$ gives the charge distribution of the ionic cores of the pseudopotentials.

The quantities $n^{\rm tst}(\mathbf{r})$ are test charge densities with the property that for $\Delta n^{\rm v}(\mathbf{r}) - n^{\rm tst}(\mathbf{r})$ the monopole and dipole moment vanish. This is useful in order to evaluate the corresponding integrals with the fast Fourier transformation technique. $V^{\rm tst}(\mathbf{r})$ is the electrostatic potential corresponding to $n^{\rm tst}(\mathbf{r})$.

The force on the bth atom, $\mathbf{F}_b = -\frac{dE^{\rm tot}}{d\mathbf{R}_b}$, contains integrals (similar to the total energy) with kernels which are localized. Details can be found in Ref. 28.

III. CHEMICAL TRENDS

In this section we describe an application of the SSGF method to a representative set of third row adatoms, namely Na, Si, and Cl, which are adsorbed on Al(111). The non-linearity of the exchange-correlation energy functional for the core and valence electrons (see Sec. II) is taken into account just for Na because only for alkali-metal atoms is the overlap of valence and core states appreciable.

First we discuss the calculated equilibrium height of the adsorbate $d_{\rm eq}$, which is defined as the distance between the adatom and the top substrate layer. The calculated total energy for Si is given for different adsorbate heights in Fig. 1, where we also show the energy as obtained from an integral of the calculated forces. The good agreement of the integrated forces and the total energy demonstrates the high numerical accuracy. In Table I we compare our results with the jellium calculations of

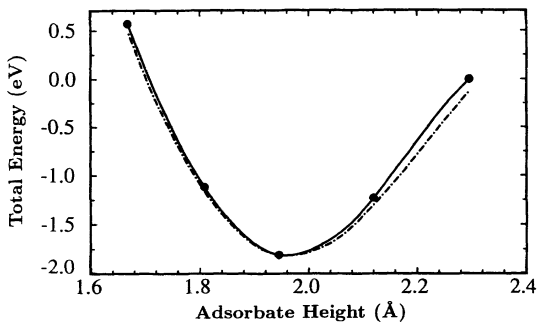

FIG. 1. Total energy as a function of the adsorbate height for Si on Al(111) at the fcc-hollow site. The $d = 0$ height is the center of the top substrate layer. The energy zero has no direct physical relevance. The dot-dashed line is obtained from integration of the calculated forces.

TABLE I. Equilibrium distances $d_{\rm eq}$ (Å) for Na, Si, and Cl (measured from the center of the top substrate layer). The results labeled jellium are from Lang and Williams.[1] Because they give adatom heights with respect to the jellium edge, we added to their numbers half an interplanar spacing of Al(111), i.e., 1.15 Å. SSGF are results obtained using the self-consistent surface-Green-function method, and PW are results obtained from supercell calculations with a plane-wave basis set and a coverage of $\Theta = 1/16$. The numbers in brackets give the corresponding adatom-Al bond lengths in Å. The radius of metallic Al is $r_{\rm Al} = 1.41$ Å.

Adsorbate	Jellium	SSGF	PW
Na	2.79	2.69 (3.14)	2.70 (3.16)
Si	2.37	1.95 (2.54)	1.80 (2.43)
Cl	2.52	2.09 (2.65)	1.92 (2.51)

Lang and Williams.[1] It shows that the jellium substrate overestimates the equilibrium distance. Whereas this error is small for the Na adsorbate ($\approx 3\%$), it is rather large for the smaller Si and Cl adatoms ($\approx 20\%$). It is interesting to note that for Si on a jellium surface and using first-order perturbation theory for the lattice, an equilibrium adatom height of 1.95 Å is obtained,[1] which is identical to our full SSGF result (see also Ref. 8). We also included in Table I the results of plane wave (PW) supercell calculations. For these calculations the substrate is described by a slab consisting of four Al layers and the vacuum region has a thickness of seven Al layers. As shown elsewhere,[4] this small number of layers gives reliable results provided one adsorbs only on one side of the slab. For the calculations a very low coverage of one adsorbate per 16 substrate-surface atoms was used. The basis set consists of plane waves with kinetic energy up to $E^{\rm cut} = 8$ Ry, and the $\mathbf{k}$ integration is replaced by one special point in the irreducible part of the Brillouin zone.[29] For details of the method we refer to Ref. 4.

The agreement between the PW and the SSGF results is good, the maximum deviation in the adatom-Al bondlength is less than 0.17 Å. We believe that the differences are due to numerical inaccuracies in the SSGF calculations which result from small inaccuracies in the charge density $n^{\rm v,0}(\mathbf{r})$ near and inside the substrate surface. Therefore, they are more acute for smaller adsorbates.

Figure 2 shows the adsorbate-induced density of states $\Delta N(\epsilon)$ for the three adsorbates as well as the density of states of aluminum. $\Delta N(\epsilon)$ is calculated from the generalized phase shift [see Eq. (10)] by[9]

$$\Delta N(\epsilon) = \frac{2}{\pi}\frac{d}{d\epsilon}\delta(\epsilon) \quad . \tag{11}$$

The main differences between Fig. 2 and the results of the $r_s = 2$ jellium substrate, which is typically called aluminum, are: (i) the theoretical band width of aluminum is 11.3 eV, and that of jellium is 12.5 eV, and (ii) the atomic-structure induced band-structure effects on the density of states of Al at the Fermi level are clearly visible in Fig. 2. With respect to the adsorption, the expected picture for chemisorbed adatoms on metal surfaces is confirmed: Atomic states of the adsorbates are

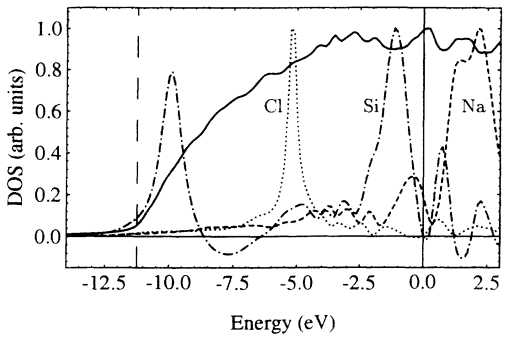

FIG. 2. Changes of the density of states, $\Delta N(\epsilon)$, induced by the adsorption of sodium (dashed line), silicon (dot-dashed line), and chlorine (dotted line) on Al(111). The density of states of the aluminum substrate is shown as a solid line. Energies are given with respect to the Fermi level, which is indicated by a vertical full line. The vertical dashed line marks the bottom of the valence band.

broadened due to the hybridization with the substrate states. The position of the Fermi level relative to the position of the broadened peaks determines the occupation of the atomic states and this determines whether the bonding should be termed ionic or covalent. The trend study of atoms from the left-hand to the right-hand side of the periodic table makes this classification much clearer than a single-case study. Thus, the $\Delta N(\epsilon)$ curve for Na where the main peak is clearly above the Fermi level is consistent with what one expects for an ionic bond where the adatom is (partially) positively charged. This result thus supports the low-coverage description of the alkali-metal adsorption given by Langmuir and Gurney[30] and by Lang and Williams.[1]

For Si the Fermi level cuts the energy range of the Si $3p$-induced peak. A detailed analysis showed, that all oscillations in $\Delta N(\epsilon)$ above the Fermi energy, which are visible in the picture, have Si $3p$ character. Thus, the Si-induced states which have bonding character with respect to the adsorbate-substrate interaction are filled and the antibonding states are empty (compare also Ref. 1). The bond is thus covalent. We emphasize that the oscillations in $\Delta N(\epsilon)$ close to the Fermi level are again a band-structure effect, and that in jellium there is only one structureless p-like resonance. The structure of this p-like adsorbate density of states (see Fig. 2) is largely determined by the clean-substrate density of states: At maxima of $\mathrm{Im}\{\mathrm{Tr}[\mathcal{G}^0(\epsilon)]\}$ we find minima of $\Delta N(\epsilon)$ and at minima of $\mathrm{Im}\{\mathrm{Tr}[\mathcal{G}^0(\epsilon)]\}$ we find maxima.

For Cl a sharp atomiclike $3p$ peak lies 5 eV below the Fermi level, and the $3s$ peak is positioned even below the metallic band at about -18 eV. This result can well be summarized by calling the adsorbed Cl negatively charged.

Comparing our results for Na, Si, and Cl with those of jellium calculations, an excellent agreement is found. Thus we conclude that the general nature of the chemical bond is described well within the jellium model of Lang and Williams.[1] The biggest differences are found for Si as the Si $3p$-induced states are cut by the Fermi level, and the atomistic substrate splits the occupied bonding and empty antibonding states.

Additional insight can be obtained from the valence-charge densities of the different adsorbate systems (see Fig. 3). In the case of sodium, the charge transfer from the adsorbate toward the substrate is clearly visible. From the vacuum side the sodium looks practically naked. Figure 3 may overemphasize this impression, because it shows a wide range of electron densities in order to be able to compare atoms from the left to the right of the periodic table. Thus, also for Na there exists (of course) a closed contour around the Na ion core, which is not shown in the figure. The first contour has a very low value that supports (again) the description of Na as being a (partially) ionized adatom and that additional particles that approach the surface will experience the "naked" side of the adsorbate. Figure 3 also shows that the electron density between the Na adatom and the Al substrate is increased. Thus, charge is displaced from the vacuum side of the Na toward the substrate side. The details of this charge transfer are much more clearly visible in the charge-density *change*, $\Delta n^{\mathrm{v}}(\mathbf{r})$, which is the quantity directly calculated by the Green-function approach and which is shown in Fig. 8 (top left). The maximum

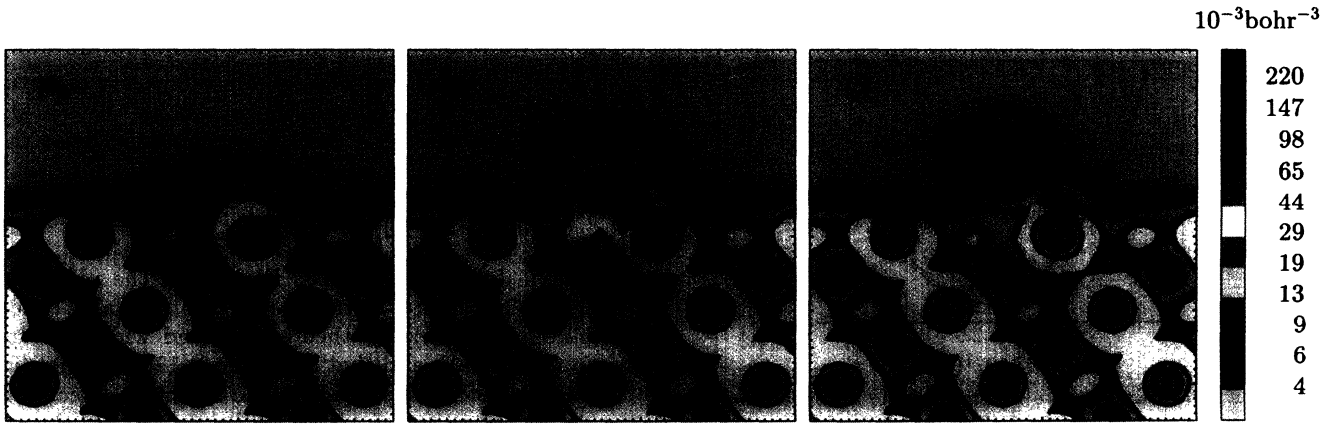

FIG. 3. From left to right, the valence-electron density for the chemisorption of sodium, silicon, and chlorine on Al(111). The contour spacing is $29 \times (1.5)^k \times 10^{-3}$ bohr^{-3}, with $-5 \leq k \leq +5$. The green-yellow border line [$k = 0, n(\mathbf{r}) = 29 \times 10^{-3}$ bohr^{-3}] is the average density of our aluminum, i.e., $r_s = 2.02$ bohr.

of $\Delta n^{v}(\mathbf{r})$ is located between the adsorbate and the substrate. In a more detailed discussion given in Sec. IV we show that the shape of this induced charge density can be understood as the response of the metallic substrate to a positively charged adsorbate. It is thus the quantum-mechanical realization of the classical image effect which is actuated by the partially ionized adsorbate.

For silicon a directed, covalent bond is visible in Fig. 3 with an increase of electron density between the Si adatom and the nearest Al atom. We also see a typical increase of electron density on the opposite side of the bonding hybrid. Thus, what was expected from the density of states is seen in the electron density. We would like to remind the reader that covalence is driven by the single-particle eigenvalues, forming occupied bonding and empty antibonding states, and the electron density $\Delta n^{v}(\mathbf{r})$ may be considered to be a result of the $\Delta N(\epsilon)$ curves and the Fermi level position. Figure 3 also shows that the bond is polarized toward the more electronegative Si, i.e., the maximum charge density of the chemisorption bond is closer to the Si nucleus.

For chlorine, a nearly spherical charge-density distribution around the adsorbate and no directed bond is found, supporting the discussion of $\Delta N(\epsilon)$ that the Cl adatom is well described as a negative ion.

IV. THE CONCEPT OF CHARGE TRANSFER

In this section we investigate the shape of the charge-density change which is induced by Na adsorption. This is essentially an elaboration of our discussion of Fig. 1 in Sec. III, and of the discussion in Ref. 9, which was concerned with Na on Al(100). We remind the reader that one driving force which determines the nature of the chemical bond is the kinetic energy operator, as this gives rise to the shell structure of atoms, and that the energy of a wave function with a node between atoms (typically called the antibonding state) has a higher single-particle energy than the wave function without a node (the bonding state). It is essentially the energy difference of the bonding state relative to the states of the uncoupled systems which determines if a bond should be called covalent or ionic. The splitting into bonding and antibonding levels together with the position of the Fermi level will be reflected in the electron density $n^{v}(\mathbf{r})$. However, investigating the density $n^{v}(\mathbf{r})$ alone will typically not give an unambiguous impression about the nature of the chemical bond.

Based on calculations for Na on jellium at a coverage of $\Theta = 1/8$, Ishida[31] recently argued that the adsorbate remains practically neutral and that the ionic picture of the chemisorption for alkali-metal atoms should be replaced by a covalent one. The analyses of several experimental studies seemed to support this conclusion. X-ray photoemission spectroscopy (XPS) measurements for alkali adsorbates on W(110) (Ref. 32) and on Ru(001) (Ref. 34) showed no shift in the binding energy of core states of the adsorbate and the substrate surface atoms with increasing coverage, while for oxygen a clear shift was observed. The interpretation was that adsorbed oxygen is partially charged, whereas for adsorbed alkali-metal atoms the charge-transfer picture should be dismissed.

Modesti *et al.*[35] found for K on Ag(001) island formation, which reflects a net attractive interaction between adsorbates. Because partially ionized alkali-metal adsorbates should give rise to a repulsive interaction, it was again concluded that the charge-transfer description is not correct. This conclusion is, however, incomplete. It is well known that with increasing coverage a strong adsorbate-adsorbate interaction sets in which is usually described in terms of a continuous compression of a homogeneous adlayer and a depolarization of the adatoms.[30,36] However, as was recently pointed out, it is also possible (and even likely) that an abrupt *phase transition* into adatom islands can occur and that this may happen already at very low coverage.[5,37,38] In these islands the nature of the chemical interactions is substantially different from the isolated adatoms because in the islands there are the adsorbate-adsorbate interactions that dominate. Thus, studying such islands, no information can be obtained about the low-coverage limit of isolated adsorbates, where only the adsorbate-substrate interaction exists.

We will now show that from a physical or chemical point of view there is no need to dismiss the concept of electronegativities and charge transfer for adsorbed atoms. As we have already used these concepts above in Sec. III, we feel that they are most valuable to summarize and understand the physical and chemical properties of adsorbates.

When a charged particle approaches a metal, a screening charge will be created at the metal surface. The quantum-mechanical realization of the classical image charge is an induced electron density at the surface which has its center of gravity at the "effective metal surface," i.e., the image plane.[1] Because electrons of an unperturbed metal surface spill out into the vacuum, the image plane is located on the vacuum side of the top substrate atomic layer. Of course, at very short distances (typically $d \lesssim 3$ Å) the justification of the image-plane concept gradually breaks down. It is still approximately valid, however, because metallic screening is still important. The concept can be approximately justified by assuming that for a charged system close to the surface the image plane is moving toward the substrate.[39] This is what we have in mind when we use the term image plane in the following discussion.

Figure 4 displays the result for a single, adsorbed Na atom. We show the *difference density*

$$n^{\Delta}(\mathbf{r}) = n^{v}(\mathbf{r}) - n^{v,0}(\mathbf{r}) - n^{\mathrm{Na},f_{3s}}(\mathbf{r}) \quad . \tag{12}$$

Here $n^{\mathrm{Na},f_{3s}}(\mathbf{r})$ is the (spherical) electron density of a partially ionized atom, where the occupation of the valence level i is given by the parameter f_i. If partial ionization of the adatom would be all that happens, then $n^{\Delta}(\mathbf{r})$ should be zero for a certain occupation number f_i. In Fig. 4 we give the result for $f_{3s} = 15\,\%$ because for this value we obtain the result that the *difference density* is practically zero on the vacuum side of the adatom. It is obvious from the figure that on the substrate side of the adatom there is an increase of electron density. According to the description favored by Ishida[31] and Riffe,

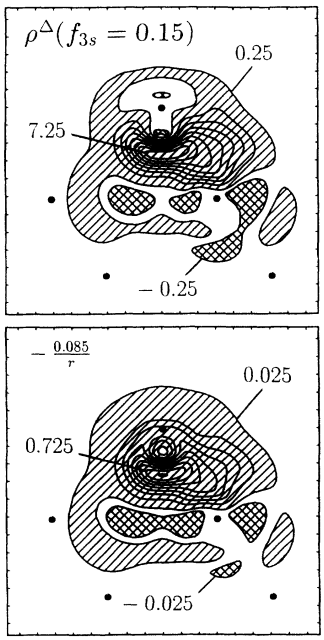

FIG. 4. *Difference density* [see Eq. (12)] for a 85% ionized sodium atom (a) and the response of the Al substrate to a negative external point charge with $q = -0.085e$ (b). Hatched regions show an increase of electron density and cross-hatched regions show a decrease. Units are 10^{-3} bohr^{-3}.

Wertheim, and Citrin,[32] the quantity $n^{\Delta}(\mathbf{r})$ is due to the polarization of the adsorbed alkali-metal atom. On the other hand, knowing that metals screen perturbations, one is tempted to associate $n^{\Delta}(\mathbf{r})$ with the metallic screening-charge density. Thus, the two different views emphasize either the adsorbate atom or the substrate as the dominant system giving rise to $n^{\Delta}(\mathbf{r})$. In order to test if the Gurney model can be kept, we have calculated the metallic screening-charge density explicitly (see also Ref. 9). For this purpose we place, at the same position where the Na ion core would sit in equilibrium, a very small charge with $q = -0.085e$, where e is the charge of one electron. This external charge induces a screening charge shown at the bottom of Fig. 4. Although the two perturbations are quite different (an external point charge with $q = -0.085e$ has no eigenfunctions in the chemically relevant energy region; its $1s$ state is at -0.1 eV) the agreement of the two figures is remarkable. Thus, the analysis of the adsorbate-induced electron density fully supports the ionic picture: The difference density $n^{\Delta}(\mathbf{r})$ can be well understood to be actuated by the metal substrate which screens the partially ionized adsorbate.

As already mentioned, the alternative interpretation which was emphasized by Ishida[31] and which has gained many followers is also consistent with the result of Fig. 4 (top). We do not question that Ishida's point of view is *in principle* (i.e., in mathematical terms) correct: If two systems A and B are brought together, the resulting bonds can be mathematically correctly described in terms of the eigenfunctions of A, or of the eigenfunctions of B, or of a combination of both. This is typically called the overcompleteness of the two Hilbert spaces of A and B. Thus, in a mathematical sense the density change in Fig. 4 can be described in terms of a linear combination of orbitals at the adsorbed atom. Then one would term the density a polarization of the adatom. Obviously it makes no sense to do this for the lower part of Fig. 4. Thus while Ishida's argument is mathematically correct, it does not describe the physical nature of the interaction. We also note that the polarization argument still requires the information and explanation of why the polarization is such that the electron increase is on the substrate side of the adatom and why a desorbed adatom leaves the surface with a certain probability as a positively charged ion. All this is naturally contained in the ionic description, which is driven by the electronegativity differences of the alkali-metal atom and the metal substrate.

In Ref. 31 Ishida determines the charge state of the adsorbate by integrating the charge density over a sphere with a radius which is more than two times larger than the ionic radius ($r_{\mathrm{Na}}^{\mathrm{Ishida}} = 2.04$ Å and $r_{\mathrm{Na}}^{\mathrm{ion}} = 0.98$ Å) and even more than 20% larger than the covalent radius of Na. Since the main part of the screening charge density lies within this sphere it is no surprise that the charge state remains practically independent of the coverage. The problem of Ishida's approach becomes obvious when it is applied to a NaCl crystal. Na is then found, for $r_{\mathrm{Na}}^{\mathrm{Ishida}}$, to be slightly *negatively* charged. This is shown in Fig. 5, where the integrated valence charge density around a Na atom in NaCl, and for a free Na atom, are plotted as a function of the sphere radius. The largest charge transfer occurs for a radius approximately equal to the ionic radius of Na, $r_{\mathrm{Na}}^{\mathrm{ion}}$. However, the absolute value is rather small ($\approx 10\%$). From Fig. 5 it is clear that the integration over a sphere can be quite misleading. This is so even for a high symmetry situation as exists in a NaCl crystal. As Fig. 3 shows, the spherical approach is even less justified for adsorbed Na.

In a more recent paper[33] Ishida also gives results of the electron charge at the adsorbed Na for smaller radii (e.g. for $r_{\mathrm{Na}} = 1.1$ Å). His low-coverage results, which correspond to a $\Theta = 1/9$ overlayer of Na on Al(111), show that for the small radii there is indeed less charge at the adsorbed Na than in a free and neutral atom (see Fig. 8 of Ref. 33). At this low coverage the adatom s resonance is only partially occupied and the adatom p_z

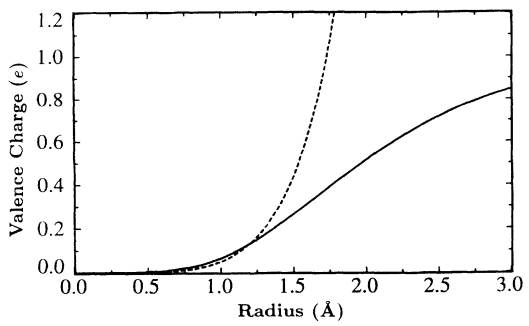

FIG. 5. Integrated charge density $Q(r) = \int_0^r n(\mathbf{r}')d^3r'$ around a free Na atom (solid line) and around a Na atom in NaCl (dashed line).

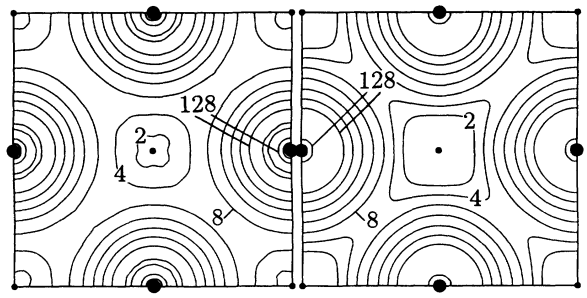

FIG. 6. Valence charge density of NaCl obtained by a superposition of the neutral atomic charge densities (left) and from a self-consistent calculation (right). The units are 10^{-3} bohr^{-3}. Large dots mark the positions of the Cl atoms, and small dots mark the Na atoms. Adjacent contour lines differ by a factor of 2. The maximum density for the non-self-consistent calculation is 265×10^{-3} bohr^{-3} and for the self-consistent calculation the highest density is 253×10^{-3} bohr^{-3}.

contribution is negligible (see Fig. 6 for $a_{\|} = 17$ and $r_s = 2$ of Ref. 33). Still, even this lowest coverage considered in Ishida's work is quite high, which is evidenced by our calculations (as well as by experiments), which show that the adatom dipole moment at $\Theta = 1/8$ is about 40% smaller than that at $\Theta \to 0$. This implies that the trend that is clearly visible in Ishida's results (see Fig. 6 in Ref. 33 for $r_s = 2$ and $a_{\|} = 8.5 \to a_{\|} = 17$) will continue toward lower coverage, which is proven by our calculations (see Fig. 7 below). As a consequence, we think that also Ishida's work confirms that at $\Theta \to 0$ the adsorbed alkali-metal adatom can be appropriately described as partially ionized.

We would also like to comment on the core-level measurements[32] which are interpreted as a clear contradiction to the ionic picture. We certainly do not argue about the experimental *results*. But we judge that the *analyses* are inappropriate. At first we note that the analyses were performed in the initial-state approximation of core-level shifts. There is clear evidence that for alkali-metal adsorbates on metal substrates this is not justified.[40–42] Even if the initial-state approximation were appropriate, we note that for alkali-metal atoms on metal substrates core-level spectroscopy does not give information about charge transfer. As Fig. 4 shows, the perturbation due to a charge outside the surface is screened before the top substrate layer is reached. In fact, as usual, close to the perturbation the screening is overdone and this is then corrected in an oscillatory way. Thus, the fact that we find a decrease of electron density close to the first substrate layer confirms the ionic model of alkali-metal adsorption and does not question it. The example of oxygen on W (100), which in the work of Riffe, Wertheim, and Citrin[32] showed the trend the authors expected for a negatively charged system, has no meaning for the study of the bigger alkali-metal atoms. The reasons are the different sign of the charge transfer and the significantly different size of the atoms. Oxygen sits too close to the surface and, therefore, for oxygen the image-plane concept is no longer applicable, while it still works (see Fig. 4) for Na.

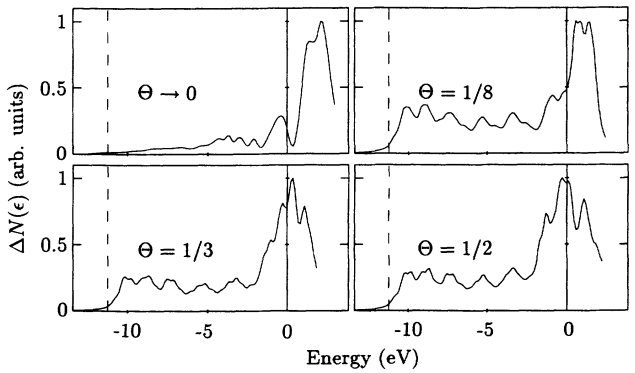

FIG. 7. Adsorbate-induced change of the density of states, $\Delta N(\epsilon)$, for Na on Al(111) for different coverages. Energies are given with respect to the Fermi level, which is indicated by a vertical full line. The vertical dashed line marks the bottom of the valence band.

For completeness of the above discussion and to demonstrate again the difficulties with the concept of charge transfer in chemically bound systems, we show in Fig. 6 the charge density of NaCl. The left part of the figure shows the result if simply *neutral* atomic densities are superimposed, and the right figure shows the result of a fully self-consistent calculation. It is obvious that the changes due to self-consistency are small and in this sense charge transfer can hardly be identified. Around the Na nucleus the charge density is only slightly decreased, and this effect is localized within the ionic radius of Na as was already shown in Fig. 5. Around the Cl atom we see that the maximum of the electron density becomes slightly lower and slightly broader in the self-consistent NaCl density when compared to the free atom densities. Thus, when one only inspects the charge density, even NaCl does not present a clear case for a system with ionic bonding. However, an analysis of the density of states shows that it is indeed appropriate to describe the upper valence band in terms of Cl p and the lower conduction band in terms of Na s orbitals. This result (again) supports the assessment that the electron density of a polyatomic system cannot be separated in a unique manner into contributions belonging to the individual atoms, and this holds for theoretical as well as for experimental studies (see also Ref. 43, pp. 27 and 324). For simple molecules, the analysis by Bader and coworkers[44] provides one possible procedure to separate the charge density and a Mulliken analysis presents a popular alternative. However, when a strong intra-atomic hybridization occurs (e.g., the formation of sp^3 orbitals) such analysis is known to fail (see Ref. 43, p. 28).

When analyzing adsorbed alkali-metal atoms, the question remains to what extent the adsorbate-substrate distance can be used to identify the nature of the bond. For alkali-metal adsorbates on Al(111) the adatom effective radius is larger than the ionic radius ($r_{\mathrm{Na}}^{\mathrm{ad}} = 1.27$ Å, see Table I; $r_{\mathrm{Na}}^{\mathrm{ion}} = 0.98$ Å). This is understandable as a consequence of the fact that in the adsorbate system one deals with two unequal partners: the adsorbate atom and the semi-infinite substrate. Therefore, the substrate

TABLE II. Dynamical charge, $\partial\mu/\partial d$, as obtained for an isolated adatom on jellium[1] and from supercell calculations (labeled PW) for adsorbates on Al(111) at a low coverage of $\Theta = 1/16$. The units are electron charges.

Adsorbate	Jellium	PW
Na	0.4	0.4
Si	0.0	−0.1
Cl	−0.5	−0.5

atoms lose, to some extent, their isolated-atom identity and the identification of the atomic radii of the substrate atoms at the substrate surface is less well defined. In fact, for a close-packed surface the adsorbate height with respect to the image plane of the substrate might be a more relevant quantity than the adsorbate-substrate interatomic distance.

A further interesting quantity obtainable in adsorbate calculations is the change of the adsorbate-induced dipole moment as a function of adsorbate height. In a naive picture one would expect that for ionic bonding the dipole moment μ changes linearly with the adatom height. For a covalent bond the dipole moment should be approximately constant (for small variations of the adsorbate height). Indeed we find that this picture works. For Na we obtain a nearly linear increase of the dipole moment with increasing adsorbate height, and for Cl we obtain a decrease. The dynamical charge, which is the slope of $\mu(d)$, is given in Table II and is in good agreement with the jellium calculations of Lang and Williams. These results support again the usefulness of the ionic pictures for Na and for Cl, and of the mainly covalent description of Si adatoms with Al(111).

V. DISCUSSION OF THE COVERAGE DEPENDENCE

In this section we give a short description of how the character of the chemisorption bond changes with coverage. For this discussion we focus on the Na adsorbate. The calculations for systems with finite coverage were performed using the plane-wave supercell approach.

As in Sec. III we begin our discussion with the adsorbate-induced density of states. Whereas the Green-function approach gives this quantity directly, the plane-wave calculations require an additional analysis. We therefore project the wave functions of the adsorbate system onto those of the free atom of the adsorbate. We used eight special **k** points in the irreducible part of the Brillouin zone of the $\Theta = 1/8$ structure and smoothed the calculated density of states by a gaussian broadening with 0.5 eV. The results, summarized in Fig. 7, show that the density of states of the adsorbate broadens and moves to lower energy with increasing coverage. Whereas for low coverages the main peak is above the Fermi level, we see that at $\Theta \approx 1/3$ the adsorbate-induced density of states is cut by the Fermi level roughly at the center of the broad peak. Thus, with increasing coverage the adsorbate becomes less charged.[36]

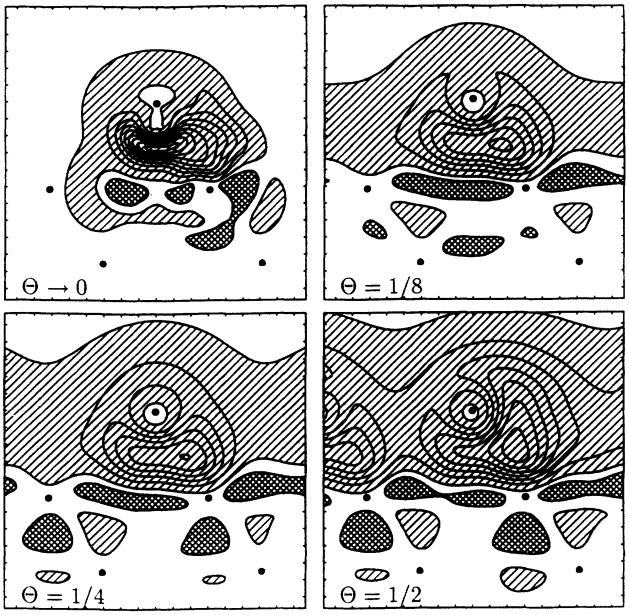

FIG. 8. Electron density for sodium on Al(111) for various coverages. The first contour lines are $+0.25 \times 10^{-3}$ bohr^{-3} (hatched regions) and -0.25×10^{-3} bohr^{-3} (cross-hatched regions) and the contour spacing is 1×10^{-3} bohr^{-3}.

This transition from a more ionic to a more metallic bond is also reflected in the adsorbate induced charge density (see Fig. 8). The strong adsorbate-adsorbate interaction due to the long-range dipole-dipole interaction also results in a significant decrease of the adsorbate-induced dipole moment with increasing coverage.[5] Even for a coverage of $\Theta = 1/8$ the dipole moment (μ = 2.6 Debye) is reduced by $\approx$ 40% with respect to the $\Theta \to 0$ result (μ = 4.0 Debye), and for $\Theta = 1/3$ (μ = 1.1 Debye) it is reduced by an additional $\approx$ 60% compared to the $\Theta = 1/8$ result.

We would like to emphasize that the coverage dependence shown in Figs. 7 and 8 (see also Refs. 31 and 33) can be calculated and has some relevance for a more general discussion. However, these results do not describe what happens in reality for Na (or K or Rb) adsorbates on Al(111). For these systems there is no continuous change from the ionic to the metallic bonding but an abrupt phase transition into a condensed phase where the adsorbates form a coexistence phase of densely packed islands and gaslike atoms in between.[5]

VI. SUMMARY

In this paper we presented self-consistent Green-function calculations for a representative set of adsorbates on Al(111). We calculated total energies, forces, the equilibrium geometry, electron density of states, electron charge density, and adsorbate induced dipole moments. When going from the left to the right of the periodic table (i.e., from the adatom Na to Si to Cl) we find that the simple description of the adatom substrate interaction in terms of the electronegativity differences

is useful. It describes well the adsorbate-induced density of states and the charge rearrangement at the surface. While the electronegativity concept is judged to be useful we also emphasize that for adsorbates it will typically not give an unambiguous quantitative description of the charge transfer. In this sense we think that the criticism of the Langmuir-Gurney picture of alkali adsorption, which can be found in the recent literature (e.g., Refs. 31–33), is built to a large extent on semantics. As discussed in Sec. IV, the electronegativity concept is useful in order to understand the density of states and the electron charge density and to impress their behavior on one's memory; but the quantitative amount of electron withdrawn or donated from one atom to another one cannot be calculated in a unique way, nor can it be measured. The Green-function calculations essentially confirm the results of Lang and Williams, who studied a jellium substrate – although some quantitative differences occur for an Al(111) substrate. Our calculation for isolated adatoms are then complemented by calculations for periodic adlayers. These results are obtained with a supercell approach. For example, they show that even at a coverage of 1/8 of a monolayer the adsorbate-adsorbate interaction for adsorbed Na is large and the adsorbate-induced dipole moment in the 1/8 adlayer is already reduced by 40% compared to that of the isolated adatom.

ACKNOWLEDGMENTS

We thank N. Lang for helpful and stimulating discussions and Li-Juan Yang, K. Kambe, and C. Stampfl for a critical reading of the manuscript.

* Permanent address: GEVAS, Frankfurter Ring 193a, D-80807 München, Germany.

† Present address: Xerox PARC, 3333 Coyote Hill Rd., Palo Alto, CA 94304.

[1] N.D. Lang and A.R. Williams, Phys. Rev. B **18**, 616 (1978).

[2] J.K. Grepstad, P.O. Gartland, and B.J. Slagsvold, Surf. Sci. **57**, 348 (1976).

[3] A. Schmalz, S. Aminpirooz, L. Becker, J. Haase, J. Neugebauer, M. Scheffler, D.R. Batchelor, D.L. Adams, and E. Bøgh, Phys. Rev. Lett. **67**, 2163 (1991).

[4] J. Neugebauer and M. Scheffler, Phys. Rev. B **46**, 16 067 (1992).

[5] J. Neugebauer and M. Scheffler, Phys. Rev. Lett. **71**, 577 (1993).

[6] For Na on Al(111) the on-surface hollow site represents a metastable geometry, which is separated from the ground state (the substitutional site) by an energy barrier of about 0.8 eV (see Ref. 4).

[7] J.N. Andersen, E. Lundgren, R. Nyholm, and M. Qvarford, Surf. Sci. **289**, 307 (1993).

[8] It is interesting to note that when the lattice is introduced to the jellium model by first-order perturbation theory and including the associated Madelung energy, the surface energy becomes nearly correct [see Lang, Solid State Phys. **28**, 225 (1973)]. This means that the use of jellium wave functions is sufficient to study the surface energy, but the density of states needs to be improved.

[9] M. Scheffler, Ch. Droste, A. Fleszar, F. Máca, G. Wachutka, and G. Barzel, Physica B **172**, 143 (1991); G. Wachutka, A. Fleszar, F. Máca, and M. Scheffler, J. Phys. C **4**, 2831 (1992).

[10] J. Bernholc, N.O. Lipari, and S.T. Pantelides, Phys. Rev. Lett. **41**, 895 (1978); Phys. Rev. B **21**, 3545 (1980).

[11] G.A. Baraff and M. Schlüter, Phys. Rev. Lett. **41**, 892 (1978); Phys. Rev. B **19**, 4965 (1979).

[12] G.A. Baraff, E.O. Kane, and M. Schlüter, Phys. Rev. B **21**, 5662 (1980).

[13] M. Scheffler, in *Festkörperprobleme XXII*, edited by P. Grosse (Vieweg, Braunschweig, 1982), p. 115.

[14] M. Scheffler, J.P. Vigneron, and G.B. Bachelet, Phys. Rev. Lett. **49**, 1765 (1982); Phys. Rev. B **31**, 6541 (1985).

[15] K. Kambe and M. Scheffler, Surf. Sci. **89**, 262 (1979); F. Máca and M. Scheffler, Comput. Phys. Commun. **51**, 381 (1988); J. Bormet, B. Wenzien, and M. Scheffler, *ibid.* **79**, 124 (1994).

[16] D.R. Hamann, M. Schlüter, and C. Chiang, Phys. Rev. Lett. **43**, 1494 (1979).

[17] G. Kerker, J. Phys. C **13**, L189 (1980).

[18] G.B. Bachelet, D.R. Hamann, and M. Schlüter, Phys. Rev. B **26**, 4199 (1982).

[19] X. Gonze, R. Stumpf, and M. Scheffler, Phys. Rev. B **44**, 8503 (1991).

[20] P.J. Braspenning, R. Zeller, A. Lodder, and P.H. Dederichs, Phys. Rev. B **29**, 730 (1984).

[21] B. Drittler, M. Weinert, R. Zeller, and P.H. Dederichs, Phys. Rev. B **39**, 930 (1989).

[22] O. Gunnarsson, O. Jepsen, and O.K. Andersen, Phys. Rev. B **27**, 7144 (1983).

[23] F. Beeler, O.K. Andersen, and M. Scheffler, Phys. Rev. Lett. **55**, 1498 (1985); Phys. Rev. B **41**, 1603 (1990).

[24] A.R. Williams, P.J. Feibelman, and N.D. Lang, Phys. Rev. B **26**, 5433 (1982).

[25] P.J. Feibelman, Phys. Rev. Lett. **35**, 2626 (1987).

[26] P.J. Feibelman, Phys. Rev. Lett. **65**, 729 (1990).

[27] D.M. Ceperley and B.J. Alder, Phys. Rev. Lett. **45**, 566 (1980).

[28] J. Bormet, Ph.D. thesis, Technische Universität Berlin, 1992.

[29] D.J. Chadi and M.L. Cohen, Phys. Rev. B **8**, 5747 (1973).

[30] R.W. Gurney, Phys. Rev. **47**, 479 (1935).

[31] H. Ishida, Phys. Rev. B **38**, 8006 (1988).

[32] D.M. Riffe, G.K. Wertheim, and P.H. Citrin, Phys. Rev. Lett. **64**, 571 (1990).

[33] H. Ishida, Phys. Rev. B **42**, 10 899 (1990).

[34] M.-L. Shek, J. Hrbek, T.K. Sham, and G.-Q. Xu, Phys. Rev. B **41**, 3447 (1990).

[35] S. Modesti, C.T. Chen, Y. Ma, G. Meigs, P. Rudolf, and F. Sette, Phys. Rev. B **42**, 5381 (1990).

[36] J.P. Muscat and D.M. Newns, J. Phys. C **7**, 2630 (1974).

[37] A.G. Naumovets, Sov. Sci. Rev. A Phys. **5**, 443 (1984).

[38] T. Aruga and Y. Murata, Prog. Surf. Sci. **31**, 61 (1989).
[39] J.A. Appelbaum and D.R. Hamann, Phys. Rev. B **6**, 1122 (1972).
[40] A.R. Williams and N.D. Lang, Phys. Rev. Lett. **40**, 954 (1978).
[41] J. Andersen (private communication); see also the discussion in Ref. 7.
[42] G.A. Benesh and D.A. King, Chem. Phys. Lett. **191**, 315 (1992).
[43] W.J. Hehre, L. Radom, P.V.R. Schleyer, and J.A. Pople, *Ab Initio Molecular Orbital Theory* (Wiley, New York, 1986).
[44] R.F.W. Bader, W.H. Henneker, and P.E. Cade, J. Chem. Phys. **46**, 3341 (1967); R.F.W. Bader, I. Keaveny, and P.E. Cade, *ibid.* **47**, 3381 (1967).

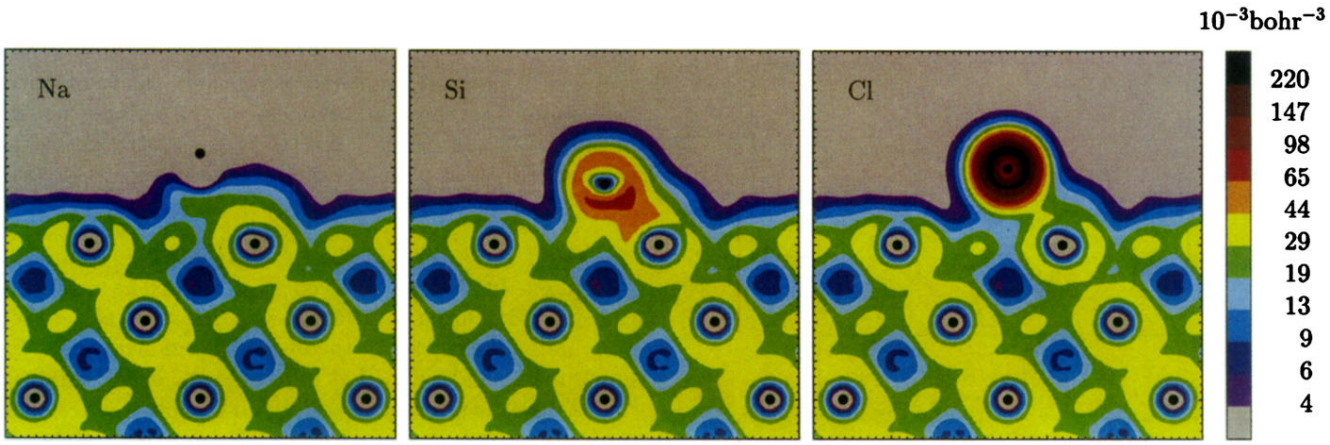

FIG. 3. From left to right, the valence-electron density for the chemisorption of sodium, silicon, and chlorine on Al(111). The contour spacing is $29 \times (1.5)^k \times 10^{-3}$ bohr^{-3}, with $-5 \leq k \leq +5$. The green-yellow border line [$k = 0, n(\mathbf{r}) = 29 \times 10^{-3}$ bohr^{-3}] is the average density of our aluminum, i.e., $r_s = 2.02$ bohr.